Magnetic fields and differential rotation on the pre-main sequence – II. The early-G star HD 141943 – coronal magnetic field, Hα emission and differential rotation

S. C. Marsden,[1,2]* M. M. Jardine,[3]* J. C. Ramírez Vélez,[4,5]* E. Alecian,[4,6]*
C. J. Brown,[7]* B. D. Carter,[7]* J.-F. Donati,[8]* N. Dunstone,[3]* R. Hart,[7]* M. Semel[4]*
and I. A. Waite[7]*

[1]*Centre for Astronomy, School of Engineering and Physical Sciences, James Cook University, Townsville 4811, Australia*
[2]*Australian Astronomical Observatory, PO Box 296, Epping NSW 1710, Australia*
[3]*SUPA, School of Physics and Astronomy, University of St Andrews, St Andrews KY16 9SS*
[4]*LESIA, Observatoire de Paris-Meudon, F-92195 Meudon Cedex, France*
[5]*Instituto de Astronomia, Universidad Nacional Autónoma de México, 04510 Coyoacan, México D.F.*
[6]*LAOG, Laboratoire d'Astrophysique de Grenoble, Université Joseph Fourier, BP 53 38041, Grenoble Cedex 09, France*
[7]*Faculty of Sciences, University of Southern Queensland, Toowoomba 4350, Australia*
[8]*LATT–UMR 5572, CNRS & Univ. de Toulouse, 14 Av. E. Belin, F–31400 Toulouse, France*

ABSTRACT

Spectropolarimetric observations of the pre-main sequence early-G star HD 141943 were made at three observing epochs (2007, 2009 and 2010). The observations were made using the 3.9-m Anglo-Australian Telescope with the UCLES echelle spectrograph and the SEMPOL spectropolarimeter visitor instrument. The brightness and surface magnetic field topologies (given in Paper I) were used to determine the star's surface differential rotation and reconstruct the coronal magnetic field of the star.

The coronal magnetic field at the three epochs shows on the largest scales that the field structure is dominated by the dipole component with possible evidence for the tilt of the dipole axis shifting between observations. We find very high levels of differential rotation on HD 141943 (∼8 times the solar value for the magnetic features and ∼5 times solar for the brightness features), similar to that evidenced by another young early-G star, HD 171488. These results indicate that a significant increase in the level of differential rotation occurs for young stars around a spectral type of early-G. We also find for the 2010 observations that there is a large difference in the differential rotation measured from the brightness and magnetic features, similar to that seen on early-K stars, but with the difference being much larger. We find only tentative evidence for temporal evolution in the differential rotation of HD 141943.

Key words: magnetic fields – stars: activity – stars: imaging – stars: individual: HD 141943.

1 INTRODUCTION

One of the key drivers of the solar dynamo is differential rotation. In the Sun strong shears occur in the interface layer between the differentially rotating outer convective zone and the inner radiative zone, which rotates as a solid body. It is these shears that help convert the large-scale solar poloidal field into a strong toroidal component. However, for young, rapidly rotating, solar-type stars a fundamentally different dynamo may be in operation.

Spectropolarimetric observations of young solar-type stars (i.e. Donati & Collier Cameron 1997; Donati 1999; Donati et al. 1999, 2003a; Marsden et al. 2006; Dunstone et al. 2008; Jeffers & Donati 2008) have shown that their reconstructed magnetic topologies have large regions of near-surface azimuthal field. These are interpreted as the toroidal component of the large-scale dynamo field in the stars. The presence of these regions near the stellar surface has led to the belief that the dynamo operating in such stars is in fact distributed throughout the stellar convective zone, rather than being restricted to the interface layer as in the solar case.

*E-mail: Stephen.Marsden@jcu.edu.au (SCM); mmj@st-and.ac.uk (MMJ); jramirez@astroscu.unam.mx (JCRV); evelyne.alecian@obs.ujf-grenoble.fr (EA); brownca@usq.edu.au (CJB); carterb@usq.edu.au (BDC); donati@obs-mip.fr (J-FD); n.j.dunstone@googlemail.com (ND); rhodes.hart@usq.edu.au (RH); Meir.Semel@obspm.fr (MS); waite@usq.edu.au (IAW)

Differential rotation is still thought to play a role in the generation of magnetic fields in these stars; however, how the dynamos in these stars operate is not well understood. Most theoretical models are based on our knowledge of the solar dynamo. The models of Kitchatinov & Rüdiger (1999) predict that the level of differential rotation on an early-G star should be greater than that on a mid-K star and that the level of surface differential rotation should decrease for stars with shorter rotational periods. While the models of Küker & Rüdiger (2005) also show that the level of differential rotation on a star should be dependent upon its effective temperature (with hotter stars having higher levels of differential rotation) but only weakly dependent on its rotation rate. These are predictions that we can now observationally test.

There are several techniques we can use to observationally measure the level of differential rotation on a star. Direct star-spot tracking from multiple Doppler images of the surface features (i.e. Collier Cameron, Donati & Semel 2002), cross-correlating two independent Doppler images (i.e. Donati & Collier Cameron 1997), incorporating a differential rotation law into the Doppler imaging process (i.e. Donati et al. 2000; Petit, Donati & Collier Cameron 2002) or by Fourier analysis of stellar line profiles (i.e. Reiners & Schmitt 2002, 2003).

Combining differential rotation measurements of a number of young solar-type stars, found using the Doppler imaging method, Barnes et al. (2005) found that the level of differential rotation increases with stellar temperature with early-G stars having higher levels of differential rotation than lower-mass stars, in agreement with the findings of Kitchatinov & Rüdiger (1999) and Küker & Rüdiger (2005). The results also showed only a weak (if any) correlation with stellar rotation rate, again in agreement with the findings of Küker & Rüdiger (2005). However, more recent measurements of the young early-G star HD 171488 (Marsden et al. 2006; Jeffers & Donati 2008; Jeffers et al. 2011) have shown this star to have an even higher level of differential rotation than that indicated by Barnes et al. (2005) with differential rotation measurements up to 10 times the current solar value. This supports the findings of Reiners (2006) which show high levels of differential rotation on a number of F stars.

A work by Donati, Collier Cameron & Petit (2003b) has shown that for some early-K stars the level of differential rotation measured from surface brightness features is consistently lower than that measured from the magnetic features (using the same data set). This has led them to surmise that this is a result of the magnetic and brightness features being anchored at different depths within the stellar convective zone and that the convective zone has a radially varying differential rotation structure, unlike the Sun. The work also showed that these early-K stars evidence temporal variation in their levels of differential rotation that the authors attribute to a feedback mechanism in the stellar dynamo periodically converting magnetic energy into kinetic energy and vice versa.

As we have mentioned above, there is currently only one early-G star for which there are differential rotation measures from both brightness and magnetic features obtained at multiple epochs, HD 171488 (Marsden et al. 2006; Jeffers & Donati 2008; Jeffers et al. 2011). This work has shown very little difference in the level of differential rotation measured from the magnetic and brightness features, although the measurement errors are larger than that found on the early-K stars (Donati et al. 2003b). Additionally, there appears to be little evidence of temporal evolution in the level of differential rotation on HD 171488. This has been speculated to be caused by the thinner convective zone of HD 171488 compared to that of the early-K stars previously studied.

Table 1. Fundamental parameters of HD 141943 from Paper I.

Parameter	value
Age	$\sim$17 Myr
Mass	$\sim$1.3 $M_\odot$
Photospheric temperature	5850 ± 100 K[a]
Spot temperature	$\sim$3950 K
Unspotted luminosity	2.8 ± 0.1 $L_\odot$ [a]
Stellar radius	1.6 ± 0.15 $R_\odot$
$v \sin i$	35.0 ± 0.5 km s^{-1}
Radial velocity (v_{rad})	$\sim$0.1 km s^{-1}
Inclination angle (i)	$70° \pm 10°$
Equatorial rotation period (P_{eq})	$\sim$2.182 d

[a]Assumed errors (see Paper I).

In order to expand the number of young early-G stars studied with spectropolarimetry this paper along with the first paper in the series Marsden et al. (2011, Paper I) and Waite et al. (2011, Paper III), presents differential rotation measurements, and magnetic maps, of two young early-G pre-main sequence (PMS) stars. Paper I deals with the reconstruction of the brightness and magnetic topologies of the star HD 141943. This paper (Paper II) presents the coronal magnetic field reconstructions, Hα activity and differential rotation measurements of HD 141943. The third paper in the series (Waite et al. 2010) deals with observations of HD 106506.

As detailed in Paper I, HD 141943 is a young, active and rapidly rotating PMS star. The stellar parameters have been determined in Paper I through the Doppler imaging process and are reproduced here in Table 1.

The reconstructed brightness images show that it has a weak polar spot and a significant amount of low-latitude spot features at all epochs. The magnetic reconstructions show that it has a predominantly non-axisymmetric radial field while its azimuthal field is predominantly axisymmetric with a ring of azimuthal field seen at the pole, similar to that of other active stars.

2 OBSERVATIONS AND DATA REDUCTION

HD141943 was observed at three epochs on the 3.9-m Anglo-Australian Telescope (AAT), in 2007 March/April, 2009 April and 2010 March/April. A fourth observation set was taken in 2006 May (see Paper I) but due to the limited nature of this set and the fact that it was only spectroscopic observations, we have not included it in our analysis here (note: a differential rotation measure was attempted on this data set but it was too limited to provide a result). The three data sets used were spectropolarimetric observations in left- and right-hand circularly polarized light taken using the University College London Echelle Spectrograph (UCLES) and the SEMPOL spectropolarimeter (Semel, Donati & Rees 1993; Donati et al. 2003a) visitor instrument.

The data were reduced using the ESPRIT (Echelle Spectra Reduction: an Interactive Tool) optimal extraction routines of Donati et al. (1997). We then used the technique of least-squares deconvolution (LSD, Donati et al. 1997) to sum the over 2600 photospheric spectral lines in each echelle spectrum in order to create a single high signal-to-noise ratio (S/N) profile for each observation. Further details of the observations, including an observing log, and the reduction process are given in Paper I.

3 RESULTS

Brightness and magnetic maps of HD 141943 were created at the three epochs through the inversion of the observed Stokes I (brightness) and Stokes V (magnetic) LSD profiles. These images and the method used to create them are given in Paper I. As an extension to these results we have measured the differential rotation on the surface of HD 141943 using these maps. We have also extrapolated the radial magnetic field map to reconstruct the coronal magnetic field of the star and we have looked at the Hα emission from the star to look for prominence activity.

3.1 Surface differential rotation

If a star is observed for a number of rotations, then the surface features will evolve under the influence of the star's surface differential rotation. The surface differential rotation on a star can be determined from both its spot/brightness features as well as from its magnetic features.

In order to measure the differential rotation on a star a simplified solar-like differential rotation law is incorporated into the imaging process:

$$\Omega(\theta) = \Omega_{eq} - d\Omega \sin^2 \theta (\text{rad d}^{-1}), \qquad (1)$$

where $\Omega(\theta)$ is the rotation rate at latitude θ, Ω_{eq} is the equatorial rotation rate and $d\Omega$ is the rotational shear between the equator and the poles (the differential rotation). The surface differential rotation is then determined by treating both Ω_{eq} and $d\Omega$ as free parameters and determining the best fit to the data using the χ^2-minimization method. This method is further described in Donati et al. (2000, 2003b) and Petit et al. (2002).

To determine the surface differential rotation usually requires that a significant part of the stellar surface be observed on at least two occasions preferably several days apart (see Petit et al. 2002). As the rotational period of HD 141943 is close to 2.2 d (see Table 1), this means that in order to determine the level of surface differential rotation the observations need to cover a time base of around a week or more. We attempted to determine the level of surface differential rotation on HD 141943 from the brightness and magnetic features in each data set. Unfortunately, the differential rotation could only be measured from the 2007 March/April magnetic data and the 2010 March/April magnetic and brightness data. The other data sets did not produce a minimum in the χ^2 landscape (see below) so the level of differential rotation could not be determined.

For the 2007 March/April magnetic data (Stokes V) the imaging code was forced to converge to a fixed magnetic field value of 91.3 G (with the level of magnetic field determined through an iterative process) for various values of Ω_{eq} and $d\Omega$. This produced the reduced χ^2 landscape shown in the upper image of Fig. 1. Fitting a paraboloid to this data gave $\Omega_{eq} = 2.882 \pm 0.009 \, \text{rad d}^{-1}$ and $d\Omega = 0.347 \pm 0.035 \, \text{rad d}^{-1}$, with the errors being 1σ errors.

For the 2010 March/April magnetic data (Stokes V) the imaging code was forced to converge to a fixed magnetic field value of 70.9 G and produced the reduced χ^2 landscape shown in the middle image of Fig. 1. Fitting a paraboloid to the central region of the data gave $\Omega_{eq} = 2.886 \pm 0.009 \, \text{rad d}^{-1}$ and $d\Omega = 0.439 \pm 0.025 \, \text{rad d}^{-1}$.

The level of differential rotation ($d\Omega$) in 2010 for the magnetic features is higher than that found in 2007, with the difference corresponding to a $\sim 2\sigma$ change. This is a marginal change, so we feel that it is only tentative evidence of temporal evolution in the differential rotation of HD 141943.
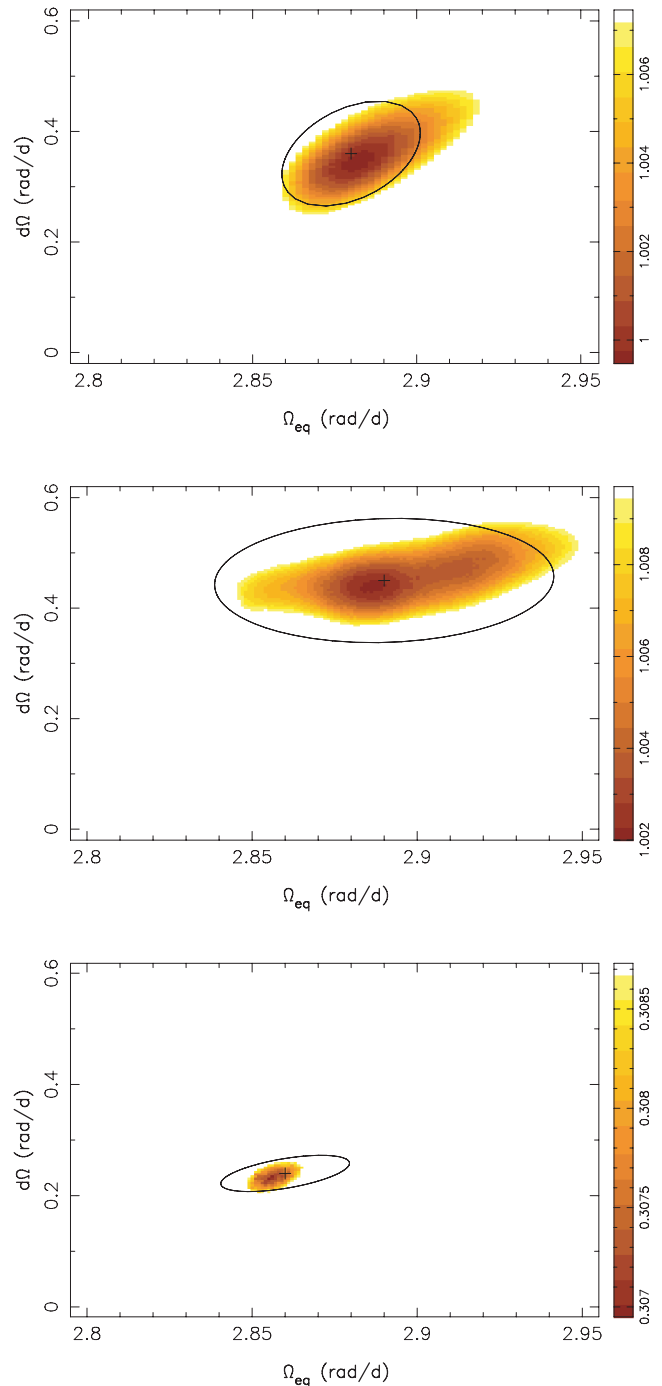

Figure 1. Surface differential rotation χ^2-minimization for HD141943, 2007 March/April Stokes V data (upper plot), 2010 March/April Stokes V data (middle plot) and 2010 March/April Stokes I data (bottom plot). The coloured images show the reduced χ^2 values obtained from the maximum-entropy imaging code for various values of Ω_{eq} and $d\Omega$ assuming that all the stellar parameters are correct. Darker regions correspond to lower reduced χ^2 values. The coloured images project to $\pm 3\sigma$ on both the axes for the upper and middle plots and $\pm 5\sigma$ for the lower plot. The overplotted ellipses show the 1σ errors (projected on to both axes) for the differential rotation measures when taking into account the errors in the stellar parameters.
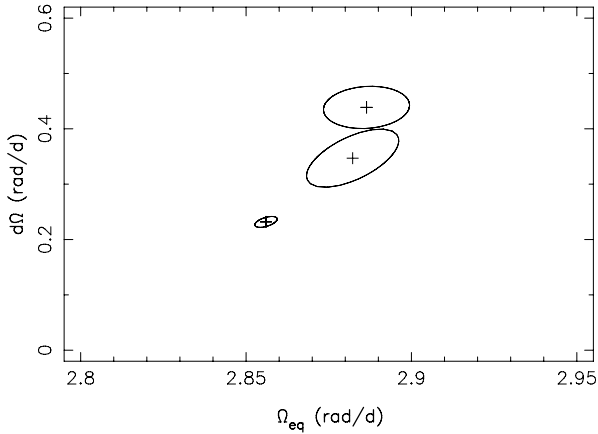
Figure 2. Plot showing the 1σ error ellipses for the surface differential rotation for HD 141943. The upper ellipse is the Stokes V data from 2010, the middle ellipse is the Stoves V data from 2007 and the bottom ellipse is the Stokes I data from 2010. These error ellipses have not taken into account the errors in the stellar parameters (see text).

For the 2010 March/April brightness data (Stokes I) the imaging code was forced to converge to a spot-filling factor of 0.029 (2.9 per cent) and produced the reduced χ^2 landscape shown in the bottom image of Fig. 1. Fitting a paraboloid gave $\Omega_{eq} = 2.856 \pm 0.002$ rad d^{-1} and $d\Omega = 0.232 \pm 0.007$ rad d^{-1}.

For 2010 the level of differential rotation from the brightness features is significantly different from that found from the magnetic features, corresponding to a $\sim 8\sigma$ change. This is a definite detection of different differential rotation rates for the brightness and magnetic features on HD 141943. Fig. 2 shows a plot of the 1σ error ellipses for all the three differential rotation measurements on the same graph.

These measures (and errors) of differential rotation assume that the stellar parameters used in the imaging code are correct and as shown in Table 1 they themselves have some uncertainty. The main parameters that will affect the measure of differential rotation are the $v\sin i$, the inclination angle and the rotational period. Taking these errors into account gave the surface differential rotation measures shown in Table 2 and also as the overplotted ellipses in Fig. 1.

The level of differential rotation for the magnetic features on HD 141943 is approximately eight times the solar differential rotation rate. While the level of differential rotation for the brightness features is approximately five times the solar value.

It should be noted that the magnetic data for 2009 April gave an extremely shallow paraboloid around $\Omega_{eq} = 2.84 \pm 0.02$ rad d^{-1} and $d\Omega = 0.0 \pm 0.1$ rad d^{-1}. However, the limited number of overlapping profiles and the poor quality of the observations early in the

Table 2. Surface differential rotation measurements for HD 141943, taking into account the errors in the stellar parameters given in Table 1.

Epoch	Ω_{eq} (rad d^{-1})	$d\Omega$ (rad d^{-1})
Stokes I (brightness)		
2010.244	2.86 ± 0.02	0.24 ± 0.03
Stokes V (magnetic)		
2007.257	2.88 ± 0.02	0.36 ± 0.09
2010.244	2.89 ± 0.05	0.45 ± 0.08

observing run (see Paper I) means that we believe this measurement of surface differential rotation to be highly suspect.

3.2 Coronal field extrapolation

The coronal magnetic fields are extrapolated from the surface magnetograms using the 'Potential Field Source Surface' method (Altschuler & Newkirk 1969; van Ballegooijen, Cartledge & Priest 1998). Since the method has been described in Jardine, Collier Cameron & Donati (2002a) we provide only an outline here. Briefly, the condition that the field is potential requires that $(\nabla \times \boldsymbol{B} = 0)$ and so we can write the magnetic field $\boldsymbol{B}$ in terms of a scalar flux function Ψ such that $\boldsymbol{B} = -\nabla\Psi$. The condition that the field is divergence-free then reduces to Laplace's equation $\nabla^2\Psi = 0$ with a solution in spherical coordinates (r, θ, ϕ):

$$\Psi = \sum_{l=1}^{N}\sum_{m=-l}^{l}[a_{lm}r^l + b_{lm}r^{-(l+1)}]P_{lm}(\theta)e^{im\phi}, \qquad (2)$$

where the associated Legendre functions are denoted by P_{lm}. The coefficients a_{lm} and b_{lm} are determined by imposing the radial field on the surface from the Zeeman–Doppler maps and by assuming that at some height R_s above the surface (known as the *source surface*) the pressure of the hot coronal gas overcomes the ability of the magnetic field to confine it. Thus, at the source surface the field lines are opened up to become purely radial, and hence $B_\theta(R_s) = B_\phi(R_s) = 0$.

We determine the plasma pressure at every point by calculating the path of the field line through that point and solving for isothermal, hydrostatic equilibrium along that path. In this case, the gas pressure is $p = p_0 e^{\frac{m}{k_B T}\int g_s \, ds}$, where m is the mean particle mass, k_B is Bolzmann's constant, T is the temperature and $p = p_0$ is the gas pressure at the base of the field line. We note that the integration in this expression is performed along the path of the field line and that $g_s = (\boldsymbol{g} \cdot \boldsymbol{B})/|\boldsymbol{B}|$ is the component of gravity along the field. We note that the plasma pressure is set to zero at any point where the field line through that point experiences a plasma pressure greater than the magnetic pressure somewhere along its length. In this case, we assume that this field line should have been forced open by the pressure of the plasma. The gas pressure at the footpoint of the field line p_0 is a free parameter of this model. Following Jardine et al. (2002a,b) we choose to scale p_0 to the magnetic pressure at the base of the field line, such that $p_0 = KB_0^2$ where K is a constant that is the same on every field line. By scaling K up or down we can scale the overall level of the coronal gas pressure and hence the density and the emission measure. Our model therefore has two parameters: the radius at which the field lines are opened up (the *source surface*) and the constant K which determines the gas pressure p_0 at the base of each field line. These two parameters determine the magnetic field structure and X-ray emission measure of the closed-field regions of the stellar corona. These are given in Fig. 3 for the three epochs.

3.3 Hα variation

The Hα line in active solar-type stars is often used as an activity indicator with the line being 'filled-in' in more active stars (i.e. Soderblom et al. 1993). In addition, prominence activity in the stellar chromosphere can also be mapped on such stars that show emission in the Hα line (i.e. Collier Cameron & Robinson 1989; Donati et al. 2000). We have analysed the Hα line of HD 141943 in 2007 March/April and 2010 March/April as the most complete
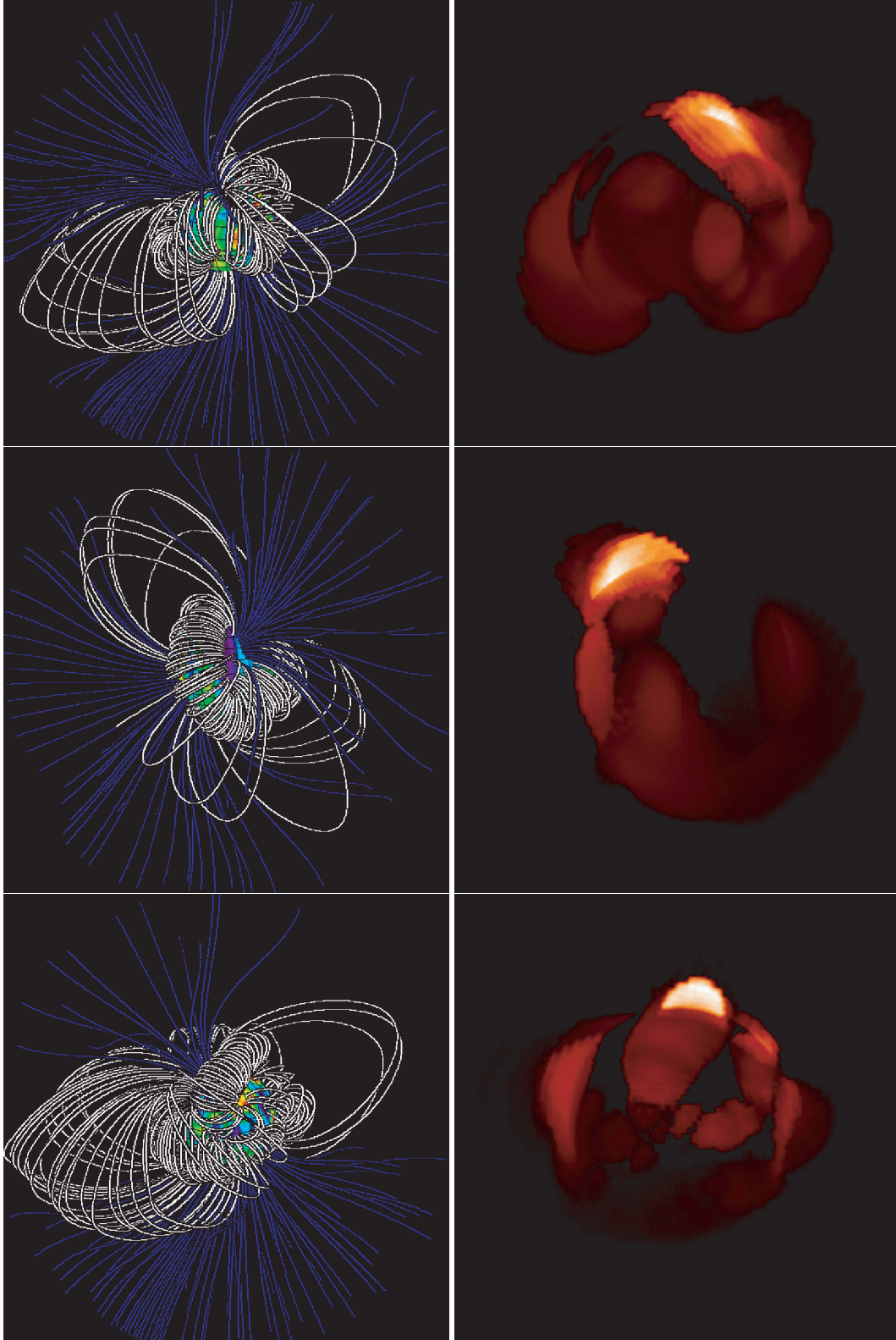
Figure 3. The images on the left are the coronal magnetic structure of HD 141943 in 2007 (upper-left), 2009 (middle-left) and 2010 (bottom-left) for a source surface of 4.8 R$_\star$. Closed field lines are shown in white while open field lines are shown in blue. The images on the right are the X-ray emission of HD 141943 in 2007 (upper-right), 2009 (middle-right) and 2010 (lower-right) for the same source surface and a coronal temperature of 2×10^7 K. All images are looking at phase 0.75 on the star.
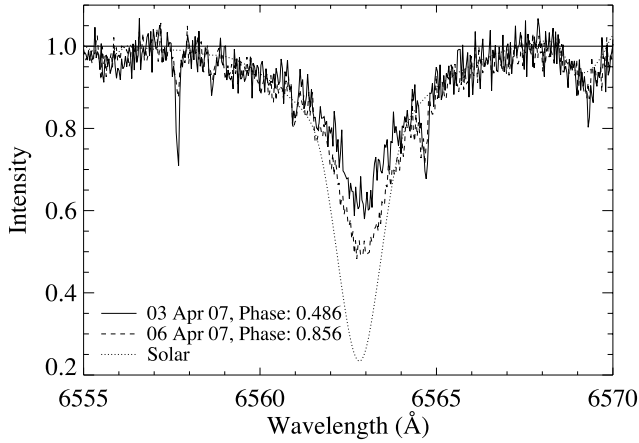
Figure 4. Plot of the Hα profile of HD141943 at two epochs in 2007 March/April along with the solar Hα profile taken with the same instrumental set-up and shifted and convolved (by the *v*sin *i* of HD 141943) to match the HD 141943 observations.

data sets to look for possible variations that may be attributable to prominence activity in the stellar chromosphere. As shown in Fig. 4, HD 141943 is a more active star than the Sun with a variable level of activity in 2007, but it does not have the overt Hα emission of a young T Tauri star.

In order to look for prominence activity on HD 141943 we have divided each of the Hα profiles in the 2007 March/April data set by the mean Hα profile from the data set. We did the same for the

2010 March/April data set, dividing by the average Hα profile from the 2010 data set. Dynamic spectra of these are displayed in Fig. 5 (2007 on the left and 2010 on the right) with darker areas showing regions of lower activity and lighter areas higher activity.

As can be seen, the Hα profile of HD 141943 in 2007 is variable in its activity level with regions of higher activity located between the phases ∼0.1 and ∼0.6 while the other phases have lower activity than average. There would appear to be some evolution in the velocity of these active/non-active regions with most of the motion restricted to within the rotational velocity of the star, although there is some enhancement/reduction of the Hα emission outside these velocities. Given the inclination angle of HD 141943, prominences located at the corotation radius of the star are likely to be seen as absorption features quickly crossing the *v*sin *i* range of the star. The absorption features seen in Fig. 5 around phase ∼0.85 appear to travel across the stellar profile, but not rapidly. A sine wave fitted to the peak/troughs of the Hα emission shows the amplitude of the sine wave to be restricted to within the *v*sin *i* of HD 141943. Thus we believe that this region is located fairly close to the surface of the star and appears to be an inactive (in Hα) low-to-mid latitude feature on, or near, the stellar surface. Comparing this to the X-ray emission image (top-right image in Fig. 3) we see that for phases around 0.0 there is little X-ray emission from the star.

For 2010 there appears to be little or no variation in the Hα emission of HD 141943. The level of Hα emission at all phases in 2010 is similar to the highest level of emission in 2007. Thus it would appear that the Hα feature seen in 2007 is not present on the star in 2010.

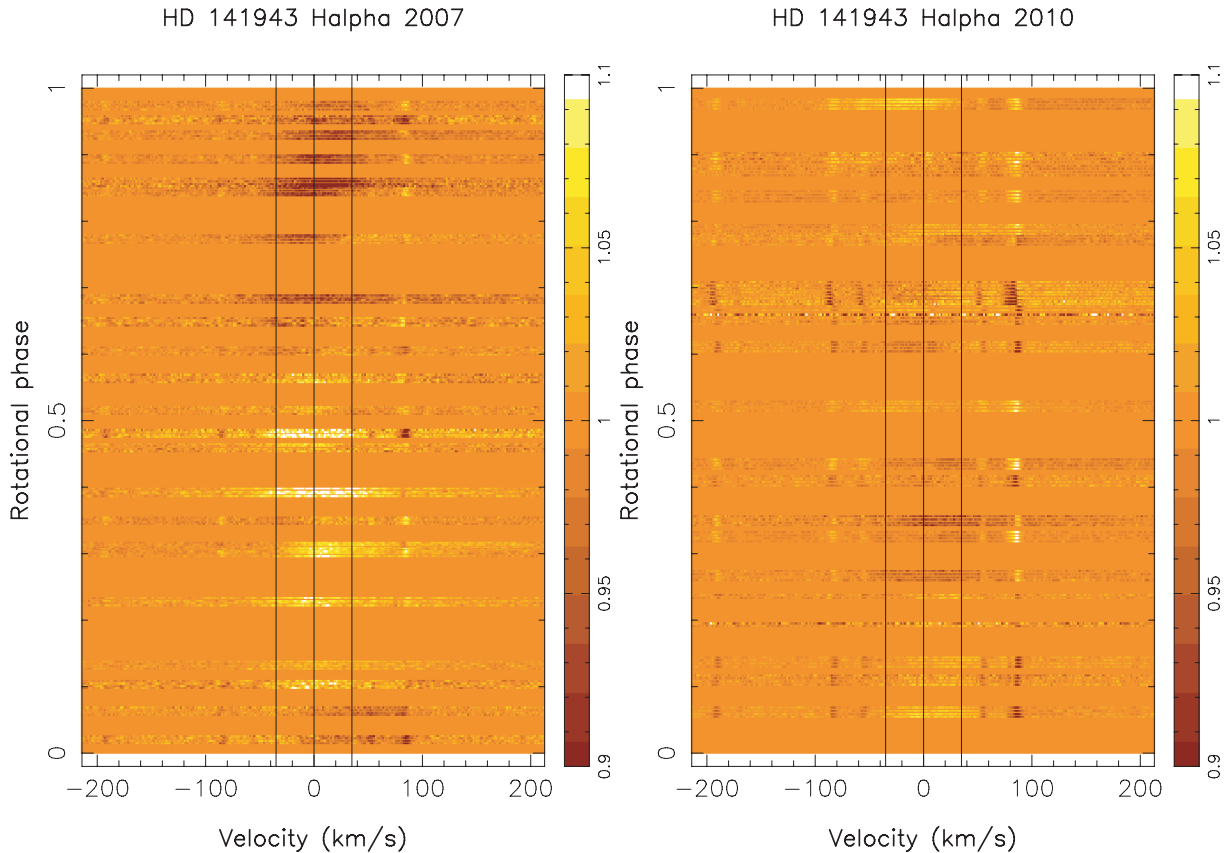**Figure 5.** Dynamic spectrum of the variation in the Hα profile of HD141943, 2007 March/April (left) and 2010 March/April (right). All the Hα profiles in each data set have been divided by the average Hα profile of each data set. The vertical thin lines represent the radial and rotational velocity of the star.

Table 3. Comparison of the stellar parameters of the five young early-G stars that have had their surface differential rotation measured using Doppler imaging. Except where noted, the data for HD 141943 come from this work and Paper I, that for HD 106506 is from Waite et al. (2011) and that for HD 171488 from Strassmeier et al. (2003), Marsden et al. (2006), Jeffers & Donati (2008) and Jeffers et al. (2011). The data for R58 come from Marsden et al. (2005a,b) and the data for LQ Lup from Donati et al. (2000). The values for the depth of the convective zone are from Siess et al. (2000). For those stars with multiple measurements of differential rotation a value has been used with error bars large enough to encompass the entire range of the observations.

Parameter	HD 141943	HD 106506	HD 171488	R58	LQ Lup
$(B - V)$	0.65^a	0.605	0.62^a	0.61^b	0.69^c
Age (Myr)	~17	$\lesssim10$	$30-50$	35 ± 5	25 ± 10
Mass ($M_\odot$)	~1.3	1.5 ± 0.1	1.20 ± 0.02	1.15 ± 0.05	1.16 ± 0.04
Radius ($R_\odot$)	1.6 ± 0.1	2.15 ± 0.26	1.15 ± 0.08	$1.18^{+0.17}_{-0.10}$	1.22 ± 0.12
Inclination ($^\circ$)	70 ± 10	65 ± 5	60 ± 10	60 ± 10	35 ± 5
Convective zone ($R_\star$)	~0.16 [0.26 $R_\odot$]	~0.22 [0.47 $R_\odot$]	~0.21 [0.24 $R_\odot$]	~0.21 [0.25 $R_\odot$]	~0.26 [0.32 $R_\odot$]
Ω_{eq} (rad d^{-1}) Stokes I	2.86 ± 0.02	4.54 ± 0.01	4.84 ± 0.14^d	11.16 ± 0.04^d	20.28 ± 0.01
Ω_{eq} (rad d^{-1}) Stokes V	2.89 ± 0.05^d	4.51 ± 0.01	4.81 ± 0.10^d	–	–
$d\Omega$ (rad d^{-1}) Stokes I	0.24 ± 0.03	0.21 ± 0.03	0.41 ± 0.16^d	0.08 ± 0.07^d	0.12 ± 0.02
$d\Omega$ (rad d^{-1}) Stokes V	0.40 ± 0.13^d	0.24 ± 0.03	0.45 ± 0.06^d	–	–

^{a}From Cutispoto et al. (2002); ^{b}from Randich (2001), dereddened value; ^{c}from Wichmann et al. (1997); ^{d}multiple observations.

4 DISCUSSION

As mentioned in Paper I, HD 141943 is only the second (or third including the results for HD 106506 by Waite et al. 2011) young early-G star for which the large-scale magnetic topology has been determined, the other being HD 171488 (Marsden et al. 2006; Jeffers & Donati 2008; Jeffers et al. 2011). In total there have been five young early-G stars for which differential rotation measures have been determined. The five stars are HD 141943, HD 171488, HD 106506, R58 (Marsden, Carter & Donati 2005a; Marsden et al. 2005b) and LQ Lup (Donati et al. 2000). The stellar parameters for all five stars have been given in Paper I. However, for ease of comparison we have given these in Table 3 and included the differential rotation results of the five stars.

4.1 Surface differential rotation

The differential rotation rate found for HD 14143 is one of the largest yet found using the Doppler imaging method and is similar to that of the other young early-G star HD 171488 (Marsden et al. 2006; Jeffers & Donati 2008; Jeffers et al. 2011). It is also similar in level to that of the more mature planet-hosting late-F star Tau Boo (Donati et al. 2008; Fares et al. 2009) and is in agreement with the findings of high levels of differential rotation on inactive F stars by Reiners (2006) using the line-profile method to measure differential rotation. However, the level of differential rotation for HD 141943 and HD 171488 are significantly above that of the other young early-G stars studied using the Doppler imaging method (see Table 3). There appears to be little difference between the stars to explain the differences in differential rotation with the possible exception of their convective zone depth.

Barnes et al. (2005) have shown that generally differential rotation increases with stellar effective temperature; however, their data set does not have any stars with a differential rotation greater than d$\Omega \sim 0.2$ rad d^{-1}. As an extension of the work of Barnes et al. (2005), we have plotted the differential rotation measured using the (Zeeman) Doppler imaging technique for these stars plus the additional stars listed in Table 3 (HD141943, HD 106506 and HD 171488). Fig. 6 plots this differential rotation against stellar convective zone depth (determined from Siess, Dufour & Forestini 2000).
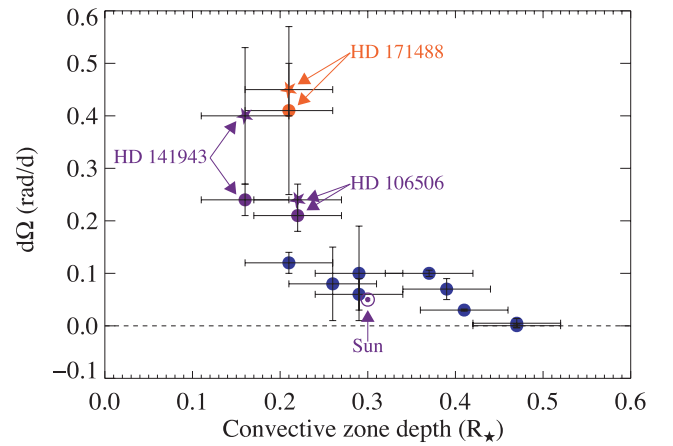

Figure 6. Differential rotation (dΩ) versus convective zone depth (as a function of stellar radius) for young solar-type stars from Barnes et al. (2005) and the new stars in Table 3. The convective zone depth has been determined from Siess et al. (2000) with an assumed error of ±0.05 R$_\star$. Dots show differential rotation measurements using brightness features and stars show differential rotation measures from magnetic features. For stars with multiple measurements a value has been used with error bars large enough to encompass the entire range of the observations.

As can be seen in Fig. 6, the level of differential rotation does appear to increase slightly with decreasing convection zones depth (with some scatter) until the convective zone depth reaches ~0.2 R$_\star$ (early-G stars) and then a dramatic increase in the level of surface differential rotation occurs. Why this should be is still not understood, but it appears that a change occurs in the rotation of the convective zone at this depth. As suggested by Jeffers & Donati (2008), for stars with thinner convective zones, such as HD 141943, we may be seeing closer to the base of the convective zone and this could explain the higher levels of differential rotation seen on these stars.

Results from Donati et al. (2003b) have shown that for early-K stars the differential rotation measured from magnetic features is higher than that measured from brightness features. They attribute this to the brightness and magnetic features being anchored at different depths in the stellar convective zone and the convective zone having a radially varying differential rotation (unlike the Sun). Jeffers & Donati (2008) and Jeffers et al. (2011) found that there is

virtually no change (within errors) in the differential rotation measured from brightness and magnetic features for the early-G star HD 171488 although the errors in the differential rotation measurements are, for the most part, much larger than the errors for the early-K stars. Although their Stokes V differential rotation measurements are for the most part higher than those measured from Stokes I. HD 106506 (Waite et al. 2011) also shows only a small increase in the differential rotation from magnetic features over that from brightness features, but again the difference is within the errors of the measurements.

In contrast to this our 2010 results for HD 141943 show a large difference between the differential rotation measured from the brightness features compared to that measured from the magnetic features, with the magnetic differential rotation being significantly higher than that from the brightness features. One possible reason for this difference could be the different latitude distributions of the brightness and magnetic features on HD 141943. In 2010 the spot features of HD 141943 are concentrated in a minor polar spot and some lower latitude features, while the magnetic features are more evenly distributed over the entire hemisphere (see fig. 5 in Paper I). Such a difference in distribution may possibly lead to biases in the determination of the differential rotation, as the differential rotation is determined over a smaller (or larger) latitude range. Both HD 106506 and HD 171488 have larger polar spots and less low-latitude spot features than HD 141943. Thus, the two stars with more dominant polar spots would be expected to be more affected by any bias in the latitude distribution between brightness and magnetic features, but neither star shows any significant disparity in differential rotation. The reason why HD 141943 alone shows a disparity in the differential rotation measurements between brightness and magnetic features remains unknown. A larger sample size is required to determine if HD 141943 is just a unique case.

Unlike the results from early-K stars (Donati et al. 2003b; Jeffers, Donati & Collier Cameron 2007) the early-G star HD 171488 shows no evidence of temporal evolution in its level of differential rotation (Marsden et al. 2006; Jeffers & Donati 2008; Jeffers et al. 2011) although again the errors are larger than the level of variation seen on early-K stars. Our magnetic results from 2007 and 2010 for HD 141943 show a slight difference (see Section 3.1), but with only a $\sim 2\sigma$ change this is only rather tentative evidence for temporal evolution in the star's differential rotation. The temporal variability seen on early-K stars is seen as evidence of a dynamo that periodically converts magnetic energy into kinetic energy, and vice versa, in the stellar convective zone. If such a mechanism is occurring in early-G stars (with thinner convective zones) it does not appear to have a large impact on the level of their differential rotation, although the errors in our differential rotation measures are too great to rule out a level of variability similar to that seen on early-K stars.

Due to the rapid winding of magnetic field lines most likely to occur on stars with high levels of differential rotation, it is possible that such stars have significantly shorter magnetic cycles than the 22-yr solar magnetic cycle. Indeed the late-F star Tau Boo does in fact appear to have a very short magnetic cycle (of ~ 2 yr, Fares et al. 2009), but this star is also the host to a 'Hot Jupiter' (Butler et al. 1997) which may also be affecting its magnetic cycle length. Both the early-G stars HD 141943 and HD 171488 have similar levels of differential rotation to that of Tau Boo and do not show any evidence of a magnetic polarity reversal over ~ 3 yr of observations (Jeffers et al. 2011; Marsden et al. 2011). So the role of differential rotation in the magnetic cycles (or if they even have cycles) of these young stars is still unknown.

4.2 Coronal magnetic field

Fig. 3 shows the structure of the coronal magnetic field and also of the X-ray emission for the 2007, 2009 and 2010 magnetic maps (see Paper I). Open field lines that would be X-ray dark and carrying the stellar wind, are shown blue, while the X-ray bright closed field lines are shown white. On the largest scales, the dipole component of the field dominates and the field structure for the three years is similar. The main change on the large scale is in the tilt of the dipole component of the field. Between 2007 and 2009, the dipole axis shifted from a latitude of 68° down to 52° and then back to 72° in 2010. On smaller scales, the field structure is very different among the three years and this is reflected in the X-ray images. As noted in Paper I the poor quality of the 2009 data set may have some role in these results.

Fig. 7 shows the magnitude and rotational modulation of the emission measure, and also the emission-measure weighted density:

$$\bar{n}_e = \frac{\int n_e^3 dV}{\int n_e^2 dV}. \tag{3}$$

These are calculated for a range of values of the base pressure, since without simultaneous X-ray observations we are unable to determine the value of the base pressure. We also show in the left column results for a model with a small corona (extending to 2.5 $R_\star$) and in the right column results for a model with a larger corona (extending to 4.8 $R_\star$). It is immediately apparent that the small changes introduced by uncertainty in the size of the corona are small compared to the changes between years. We expect the corona to be populated with loops at a range of temperatures, but in the absence of any data that might determine the nature of the differential emission measure, we take the simplest approach. We therefore show the results for a corona at a uniform temperature of 2×10^6 K and for comparison, one at a uniform temperature of 2×10^7 K.

As it might be expected, at the lower temperatures, the densities and emission measures reach higher values. The range of values is however similar for all the years and is typical of active stars. The largest difference among the three years is in the arrangement of the smaller scale loops and this results in a significant increase in the X-ray rotational modulation in 2009.

5 CONCLUSIONS

We have extrapolated the coronal magnetic field of HD 141943 from surface magnetograms acquired at three epochs. These show that the large-scale field structure of the corona is dominated by a dipole component with the axis of the dipole shifting among the three epochs. The small-scale structure shows an increase in the modelled rotational X-ray modulation in 2009, compared to the other epochs (2007 and 2010).

The surface differential rotation of HD 141943 has been measured at two epochs (2007 and 2010) from both the surface brightness features (2010) and the surface magnetic features (2007 and 2010). The differential rotation measured from the magnetic features is one of the highest values of differential rotation measured on a young solar-type star and is similar in level to the other young early-G star HD 171488, but higher than the more swollen star HD 106506. We thus conclude that the depth of the stellar convective zone plays a strong role in the level of surface differential rotation seen on solar-type stars, with a large increase in differential rotation seen for stars with convective zone depths shallower than ~ 0.2 $R_\star$.
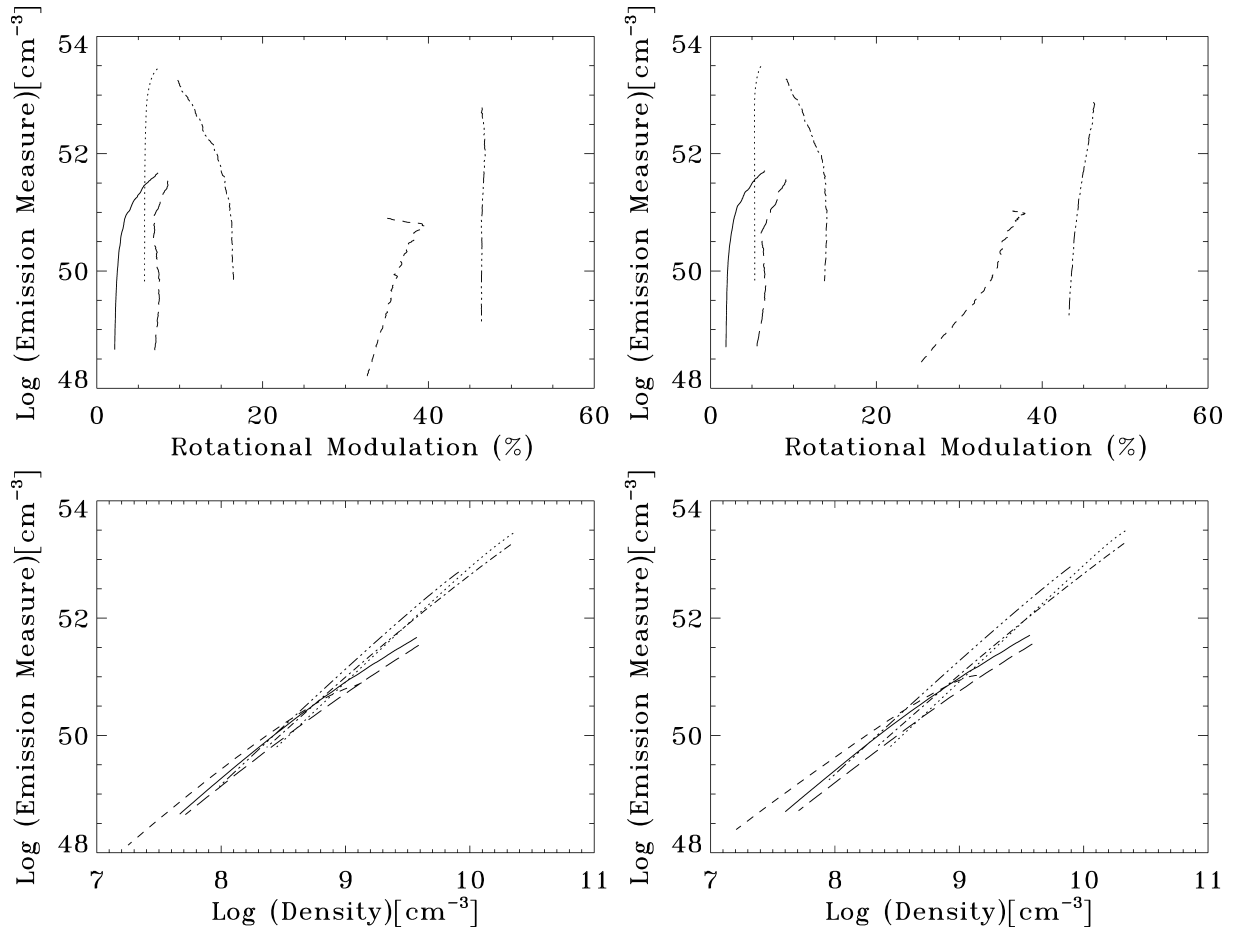
Figure 7. Emission measure for a range of models with varying rotational modulation of the emission measure (top) and also varying densities (bottom). The left-hand column shows results for the smaller corona (extending to 2.5 R$_\star$) while the right-hand column shows results for the larger corona (extending to 4.8 R$_\star$). The line styles denote different temperatures and data from different years. Thus we have the following: 2007, $T = 2 \times 10^6$ K (dotted); 2007, $T = 2 \times 10^7$ K (solid); 2009, $T = 2 \times 10^6$ K (triple-dot–dashed); 2009, $T = 2 \times 10^7$ K (short dashed), 2010, $T = 2 \times 10^6$ K (dot–dashed) and 2010, $T = 2 \times 10^7$ (long dashed).

The 2010 data set for HD 141943 shows a large increase in the level of differential rotation measured from magnetic features to that measured from brightness features. This is similar to that seen on early-K stars but with a much greater difference and is in contrast to the results from other early-G stars which show little or no difference between the differential rotation measured from brightness and magnetic features. Our results only find tentative evidence for temporal evolution in the differential rotation of HD 141943. These results when combined with those from the early-G star HD 171488 (which shows no evidence of temporal evolution in differential rotation) imply that early-G stars do not undergo large-scale evolution in their differential rotation. However, the errors in our measurements are too large to rule out small-scale evolution in differential rotation similar to that seen on early-K stars.

HD 141943 and stars of similar spectral type warrant further observations to determine what effect a shallow convective zone has on the differential rotation levels of such stars and indeed if they do show temporal evolution of their differential rotation as seen on early-K stars.

ACKNOWLEDGMENTS

REFERENCES

Altschuler M. D., Newkirk G., Jr, 1969, Solar Phys., 9, 131
Barnes J. R., Collier Cameron A., Donati J.-F., James D. J., Marsden S. C., Petit. P., 2005, MNRAS, 357, L1
Butler R. P., Marcy G. W., Williams E., Hauser H., Shirts P., 1997, ApJ, 474, L115
Collier Cameron A., Robinson R. D., 1989, MNRAS, 236, 57
Collier Cameron A., Donati J.-F., Semel M., 2002, MNRAS, 330, 699
Cutispoto G., Pastori L., Pasquini L., de Medeiros J. R., Tagliaferri G., Anderson J., 2002, A&A, 384, 491
Donati J.-F., 1999, MNRAS, 302, 457
Donati J.-F., Collier Cameron A., 1997, MNRAS, 291, 1
Donati J.-F., Semel M., Carter B. D., Rees D. E., Cameron A. C., 1997, MNRAS, 291, 658
Donati J.-F., Collier Cameron A., Hussain G., Semel M., 1999, MNRAS, 302, 437

Donati J.-F., Mengel M., Carter B. D., Marsden S., Collier Cameron A., Wichmann R., 2000, MNRAS, 316, 699

Donati J.-F. et al., 2003a, MNRAS, 345, 1145

Donati J.-F., Collier Cameron A., Petit P., 2003b, MNRAS, 345, 1187

Donati J.-F. et al., 2008, MNRAS, 385, 1179

Dunstone H. J., Hussain G. A. J., Collier Cameron A., Marsden S. C., Jardine M., Stempels H. C., Ramirez Vlez J. C., Donati J.-F., 2008, MNRAS, 387, 481

Fares R. et al., 2009, MNRAS, 398, 1383

Jardine M., Collier Cameron A., Donati J.-F., 2002a, MNRAS, 333, 339

Jardine M., Wood K., Collier Cameron A., Donati J.-F., Mackay D. H., 2002b, MNRAS, 336, 1364

Jeffers S. V., Donati J.-F., 2008, MNRAS, 390, 635

Jeffers S. V., Donati J.-F., Collier Cameron A., 2007, MNRAS, 375, 567

Jeffers S. V., Donati J.-F., Alecian E., Marsden S. C., 2011, MNRAS, 411, 1301

Kitchatinov L. L., Rüdiger G., 1999, A&A, 344, 911

Küker M., Rüdiger G., 2005, Astron. Nachr., 326, 265

Marsden S. C., Carter B. D., Donati J.-F., 2005a, in Favata F., Hussain G. A. J., Battrick B., eds, ESA Special Publ. Vol. 560, Proc. 13th Cambridge Workshop Cool Stars, Stellar Syst. Sun. ESA, Noordwijk, p. 799

Marsden S. C., Waite I. A., Carter B. D., Donati J.-F., 2005b, MNRAS, 359, 711

Marsden S. C., Donati J.-F., Semel M., Petit P., Carter B. D., 2006, MNRAS, 370, 468

Marsden S. C. et al., 2011, MNRAS, doi:10.1111/j.1365-2966.2011.18367.x (Paper II)

Petit P., Donati J.-F., Collier Cameron A., 2002, MNRAS, 334, 374

Randich S., 2001, A&A, 377, 512

Reiners A., 2006, A&A, 446, 267

Reiners A., Schmitt J. H. M. M., 2002, A&A, 384, 155

Reiners A., Schmitt J. H. M. M., 2003, A&A, 398, 647

Semel M., Donati J.-F., Rees D. E., 1993, A&A, 278, 231

Siess L., Dufour E., Forestini M., 2000, A&A, 358, 593

Soderblom D. R., Stauffer J. R., Hudon J. D., Jones B. F., 1993, ApJS, 85, 315

Strassmeier K. G., Pichler T., Weber M., Granzer T., 2003, A&A, 411, 595

van Ballegooijen A., Cartledge N., Priest E., 1998, ApJ, 501, 866

Waite I. A. et al., 2011, MNRAS, doi:10.1111/j.1365-2966.2011.18366.x (Paper III)

Wichmann R., Krautter J., Covino E., Alcalá J. M., Neuhäuser R., Schmitt J. H. M. M., 1997, A&A, 320, 185

This paper has been typeset from a TEX/LATEX file prepared by the author.